Application of Bayesian Statistics to Muon Track Reconstruction in AMANDA

Tyce DeYoung
Santa Cruz Institute for Particle Physics, University of California, Santa Cruz, CA 95064, USA

Gary C. Hill
Dept. of Physics, University of Wisconsin, Madison, WI 53706, USA

for the AMANDA Collaboration:

X. Bai[1], G. Barouch[11], S.W. Barwick[8], R.C. Bay[7], T. Becka[9], K.-H. Becker[2], D. Bertrand[3], F. Binon[3], A. Biron[4], J. Booth[8], O. Botner[13], A. Bouchta[4*], M.M. Boyce[11], S. Carius[5], A. Chen[11], D. Chirkin[7,2], J. Conrad[13], J. Cooley[11], C.G.S. Costa[3], D.F. Cowen[10], E. Dalberg[14,17†], C. De Clercq[15], T. DeYoung[11‡], P. Desiati[11], J.-P. Dewulf[3], P. Doksus[11], J. Edsjö[14], P. Ekström[14], T. Feser[9], J.-M. Frère[3], T.K. Gaisser[1], M. Gaug[4§] A. Goldschmidt[6], A. Hallgren[13], F. Halzen[11], K. Hanson[10], R. Hardtke[11], M. Hellwig[9], H. Heukenkamp[4], G.C. Hill[11], P.O. Hulth[14], S. Hundertmark[8], J. Jacobsen[6], A. Karle[11], J. Kim[8], B. Koci[11], L. Köpke[9], M. Kowalski[4], J.I. Lamoureux[6], H. Leich[4], M. Leuthold[4], P. Lindahl[5], I. Liubarsky[11], P. Loaiza[13], D.M. Lowder[7¶] J. Madsen[12], P. Marciniewski[13], H.S. Matis[6], C.P. McParland[6], T.C. Miller[1**], Y. Minaeva[14], P. Miočinović[7], P.C. Mock[8,20††], R. Morse[11], T. Neunhöffer[9], P. Niessen[4,15], D.R. Nygren[6], H. Ögelman[11], Ph. Olbrechts[15], C. Pérez de los Heros[13], A.C. Pohl[5] R. Porrata[8‡‡] P.B. Price[7], G.T. Przybylski[6], K. Rawlins[11], C. Reed[8§§], W. Rhode[2], M. Ribordy[4], S. Richter[11], J. Rodríguez Martino[14], P. Romenesko[11], D. Ross[8], H.-G. Sander[9], T. Schmidt[4], D. Schneider[11], R. Schwarz[11], A. Silvestri[2,4], M. Solarz[7], G.M. Spiczak[12], C. Spiering[4], N. Starinsky[11¶¶], D. Steele[11], P. Steffen[4], R.G. Stokstad[6], O. Streicher[4], K.-H. Sulanke[4], I. Taboada[10], L. Thollander[14], T. Thon[4], S. Tilav[1], M. Vander Donckt[3], C. Walck[14], C. Weinheimer[9], C.H. Wiebusch[4***], R. Wischnewski[4], H. Wissing[4], K. Woschnagg[7], W. Wu[8], G. Yodh[8], S. Young[8]

[1] *Bartol Research Institute, University of Delaware, Newark, DE 19716, USA*
[2] *Fachbereich 8 Physik, BUGH Wuppertal, D-42097 Wuppertal, Germany*
[3] *Université Libre de Bruxelles, Science Faculty CP230, Boulevard du Triomphe, B-1050 Brussels, Belgium*
[4] *DESY-Zeuthen, D-15735 Zeuthen, Germany*
[5] *Dept. of Technology, Kalmar University, S-39182 Kalmar, Sweden*
[6] *Lawrence Berkeley National Laboratory, Berkeley, CA 94720, USA*
[7] *Dept. of Physics, University of California, Berkeley, CA 94720, USA*
[8] *Dept. of Physics and Astronomy, University of California, Irvine, CA 92697, USA*
[9] *Institute of Physics, University of Mainz, Staudinger Weg 7, D-55099 Mainz, Germany*
[10] *Dept. of Physics and Astronomy, University of Pennsylvania, Philadelphia, PA 19104, USA*
[11] *Dept. of Physics, University of Wisconsin, Madison, WI 53706, USA*
[12] *Physics Department, University of Wisconsin, River Falls, WI 54022, USA*
[13] *Division of High Energy Physics, Uppsala University, S-75121 Uppsala, Sweden*
[14] *Dept. of Physics, Stockholm University, SCFAB, SE-10691 Stockholm, Sweden and*
[15] *Vrije Universiteit Brussel, Dienst ELEM, B-1050 Brussel, Belgium*

(Dated: March 14, 2002)

---

[*] now at CERN, CH-1211, Genève 23, Switzerland
[†] now at Defense Research Establishment (FOA), S-17290 Stockholm, Sweden
[‡] now at Santa Cruz Institute for Particle Physics, University of California, Santa Cruz, CA 95064
[§] now at IFAE, 08193 Barcelona, Spain
[¶] now at MontaVista Software, 1237 E. Arques Ave., Sunnyvale, CA 94085, USA
[**] now at Johns Hopkins University, Applied Physics Laboratory, Laurel, MD 20723, USA
[††] now at Optical Networks Research, JDS Uniphase, 100 Willowbrook Rd., Freehold, NJ 07728-2879, USA
[‡‡] now at L-174, Lawrence Livermore National Laboratory, 7000 East Ave., Livermore, CA 94550, USA
[§§] Dept. of Physics, Massachussetts Institute of Technology, Cambridge, MA USA
[¶¶] now at SNO Institute, Lively, ON, P3Y 1M3 Canada
[***] now at CERN, CH-1211, Genève 23, Switzerland

The AMANDA neutrino telescope detects neutrinos by observing Cherenkov light from secondary leptons produced in charged current neutrino interactions. At lower energies, a background of penetrating muons approximately 10^6 times as numerous as neutrino-induced muons is rejected by looking for muons travelling upward through the earth. A comparison of maximum likelihood and Bayesian approaches to track reconstruction will be presented, and the implications of each approach for background rejection are discussed.

I. THE AMANDA DETECTOR

The Antarctic Muon and Neutrino Detector Array (AMANDA) is designed to detect secondary leptons produced in high energy neutrino charged-current interactions with the South Polar ice cap or the bedrock below. As shown in Fig. 1, the leptons are detected through the Cherenkov light emitted as they pass through the ice, which is extremely transparent. The detector presently consists of a three-dimensional array of 677 optical modules (OMs — essentially photomultiplier tubes inside glass pressure vessels) occupying a rough cylinder of 100 m radius at depths of 1500 to 2000 m below the surface of the ice cap, as shown in Fig. 2. The discussion presented here is based on data from 1997, when only the central 10 strings of the array, some 302 OMs, had been installed.

Because the high energy neutrinos the instrument is intended to detect are rare and the neutrino interaction cross section is low, an extremely large volume of ice must be monitored to achieve reasonable event rates. Monetary considerations then require the inter-OM spacing to be quite large: OMs typically are spaced by 10–20 m vertically and 20–50 m horizontally. These spacings can be compared to the optical parameters of the ice, which has a typical absorption length of around 95 m and an effective scattering length of 20–30 m [1, 2].

Although the detector is sensitive to all lepton flavors, the vast majority of AMANDA triggers are produced by muons of relatively low energy (10's to 100's of GeV at the detector). Nearly all of these muons are produced in air showers above the South Pole and penetrate to the detector. However, muons that decay in flight before reaching the surface produce high energy neutrinos, which will occasionally interact near

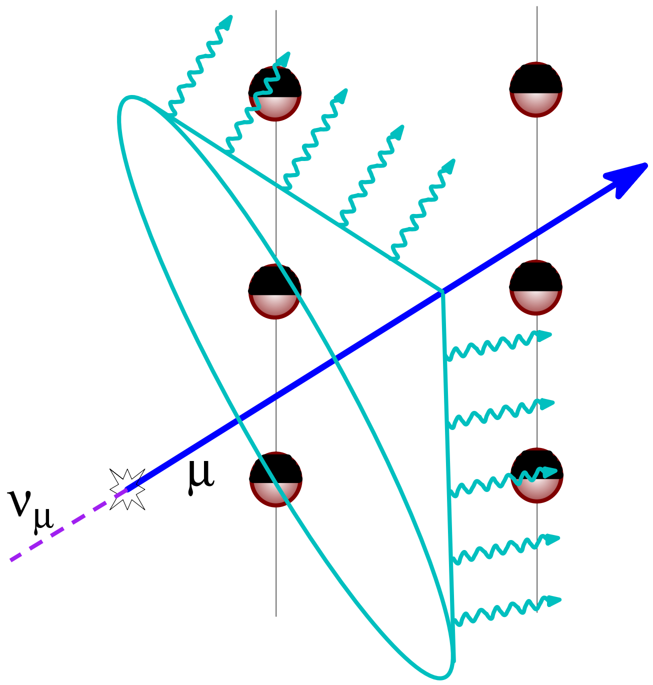

FIG. 1: Detection of the Cherenkov cone of a relativistic muon by a grid of optical modules.

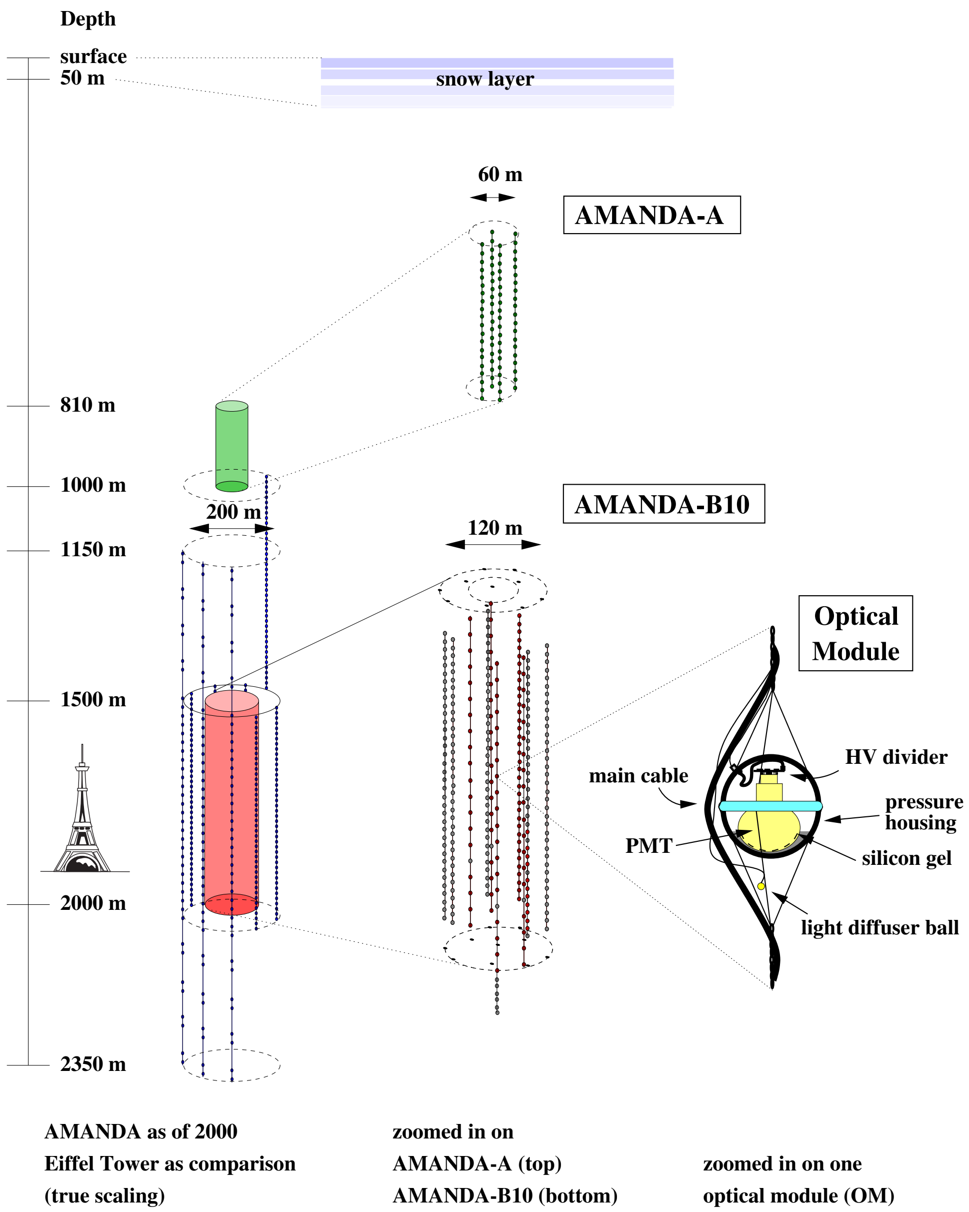

FIG. 2: The present AMANDA detector, with the Eiffel Tower shown to illustrate the scale. This paper describes data taken in 1997, using the ten inner strings labeled AMANDA-B10, shown in expanded view in the center.

the detector to regenerate the muons. For air showers above Antarctica these neutrino-induced muons are buried in the direct muon flux, but neutrino-induced muons can be observed from air showers in the Northern Hemisphere as well. The angular distributions of muons produced directly ("atmospheric muons") and those regenerated from muon neutrinos ("atmospheric neutrino events") are shown in Fig. 3.

II. TRACK RECONSTRUCTION

The sparsity of the detector array means that most low energy muons produce signals ("hits") in relatively few OMs. Typical events consist of 15–30 hits over the several hundred meters of the track. Furthermore, the low absorption of ice relative to the scattering length means that many of the photons collected are highly scattered, arriving well after the Cherenkov time (i.e., the time at which photons emitted at the

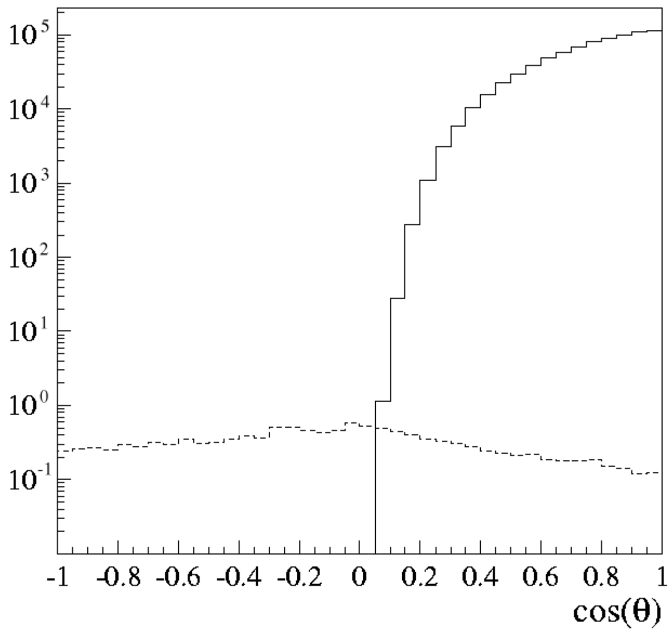

FIG. 3: Zenith angle distribution of simulated AMANDA muon events. The solid line represents penetrating downgoing muons from cosmic ray air showers [3] over Antarctica, simulated by *CORSIKA* [4] and propagated by *mudedx* [5, 6]. The dashed line indicates muons regenerated from neutrinos produced in air showers [9], simulated by *nusim* [10, 11].

Cherenkov angle and travelling in a straight line would have been observed). The relative fraction of "direct" (unscattered) photons decreases with distance from the track, as shown in Fig. 4. Because the delay time distributions are highly asymmetric, AMANDA has historically used a maximum likelihood method to reconstruct the muon track parameters from the observed time delays of the hits.

The time delay pdf's illustrated in Fig. 4 are calculated by simulating the propagation of photon fields produced by muons in ice, including the effects of scattering and absorption [7] and of the hardware response [8]. A timing likelihood

$$\mathcal{L} = \prod_{i=1}^{N_{\rm hit}} p(t_{\rm res}^{(i)} \,|\, d_\perp^{(i)}, \theta_{\rm ori}^{(i)}) \tag{1}$$

is then constructed, where $t_{\rm res}$ is the time residual, and $d_\perp$ and $\theta_{\rm ori}$ are the distance and orientation of the OM relative to the muon track, which are dependent on the parameters (x, y, z, θ, ϕ) of the muon track. For computational simplicity the probability that an OM be hit is normally not included, nor is any correction made for the bias introduced if multiple photons are detected by a single OM. The track is reconstructed by varying the muon track parameters until the minimum of the likelihood function is found. Fig. 5 shows a reconstructed muon track from the 1997 data. This event, with 41 hits, is slightly brighter than the typical muon event.

III. BACKGROUND REJECTION

Fig. 6 shows the reconstructed zenith angle distribution of AMANDA triggers. (This plot is based on data taken in 2000 with the full 19-string detector; data from 1997 are similar.) Comparison with Fig. 3 indicates that there are approximately $2 \cdot 10^3$ times as many upgoing events as expected; clearly, a large fraction of the apparently upgoing tracks are in fact misreconstructed downgoing muons.

There are several approaches that can be taken to the problem of rejecting the background of misreconstructed downgoing muons. Because of the complexity of the task, and to increase the robustness of

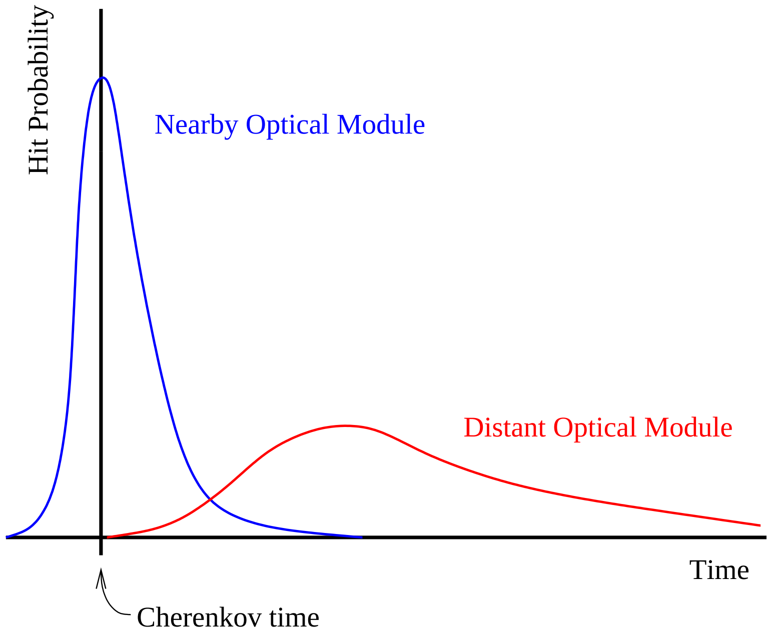

FIG. 4: Cartoon sketch of time residual (delay) distributions of photons arriving at an optical module near the muon track, compared to a distant OM. Times are relative to the arrival time expected for photons in the Cherenkov cone, and the distributions are smeared by the approximately Gaussian jitter in the response of the PMT and electronics. As the distance from the muon track increases, scattering becomes more important.

the results, two separate analyses of the data using different methods were undertaken by the AMANDA collaboration. The analyses will be only sketched out here; details are available in [12].

A. Improved Maximum Likelihood

In the first analysis, cuts were applied in several parameters indicative of accurately reconstructed muon tracks, reducing the data set by a factor of approximately 10^5. At this point, a more complete likelihood function

$$\mathcal{L}^{\rm MPE} = \mathcal{L}^{\rm MPE}_{\rm time} \cdot \mathcal{L}_{\rm hit} \tag{2}$$

was constructed and used to refit the surviving tracks. Here $\mathcal{L}^{\rm MPE}_{\rm time}$ is the timing likelihood of Eq. 1, save that the probability function is corrected for sampling bias in the case of multiple photoelectrons:

$$p(t_{\rm res}\,|\,d_\perp,\theta_{\rm ori}) \;\longrightarrow\; N\cdot p(t_{\rm res}\,|\,d_\perp,\theta_{\rm ori})\cdot\left(\int_{t_{\rm res}}^{\infty} p(t'\,|\,d_\perp,\theta_{\rm ori})\,dt'\right)^{(N-1)}$$

where N is the total number of photoelectrons detected. The hit likelihood

$$\mathcal{L}_{\rm hit} = \prod_{i=1}^{N_{\rm hit}} P(d_\perp^{(i)},\theta_{ori}^{(i)}) \;\cdot \prod_{i=N_{\rm hit}+1}^{N_{\rm OM}} \left(1 - P(d_\perp^{(i)},\theta_{ori}^{(i)})\right)$$

is just the probability that the hit tubes be hit, and that quiet tubes not be hit (regardless of time delay), in the given event [13]. This improved likelihood fit further reduced the number of misreconstructed tracks, and with the application of some additional track-quality cuts a nearly pure sample of atmospheric neutrino events was obtained, as seen in Fig. 7 [12, 14].

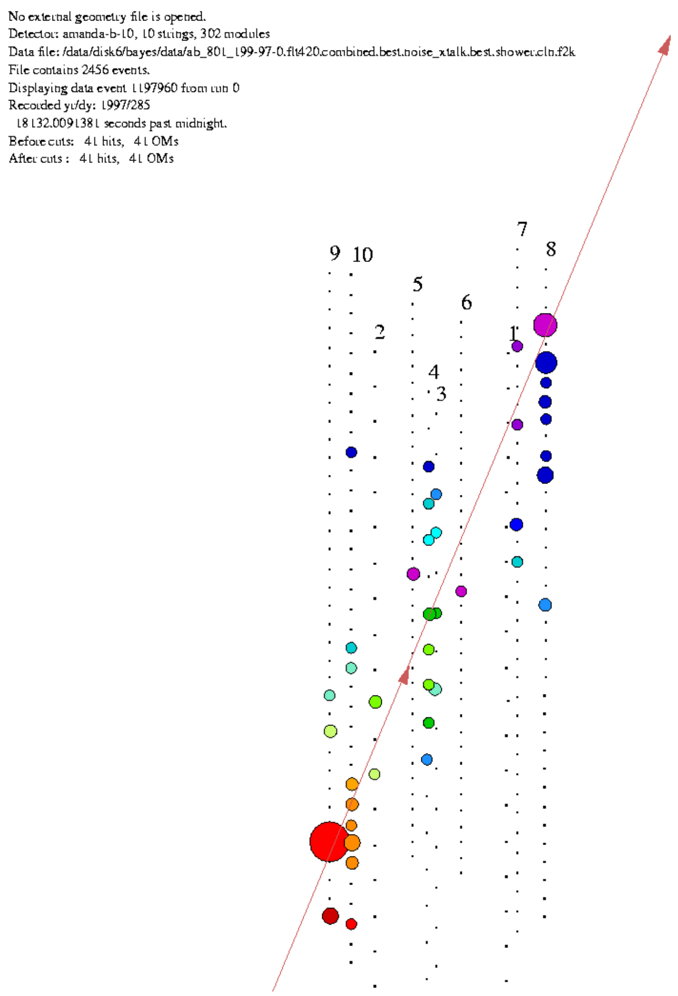

FIG. 5: An upgoing muon track recorded in 1997. The dots indicate OMs in the 10-string AMANDA detector; larger colored circles show OMs that detected light from the muon track. The size of the circles indicates the amplitude of the PMT signal, and the colors indicate the relative timing, from red (early hits) through green to purple (the latest hits). The line marks the reconstructed muon track.

B. Bayesian Reconstruction

The second analysis took a more Bayesian approach to track reconstruction. For a particular muon track hypothesis $\mu = \mu(x, y, z, \theta, \phi)$, Bayes' Theorem states that

$$P(\mu \,|\, \mathrm{data}) = \mathcal{L}(\mathrm{data} \,|\, \mu)\; P(\mu),$$

ignoring the normalization factor $P(\mathrm{data})$, which is a constant for the observed event. Here $\mathcal{L}$ is the likelihood of Eq. 1 (or, better, Eq. 2), and $P(\mu)$ is function incorporating our prior knowledge of the muon flux to which AMANDA is exposed. The most important feature of that flux is its zenith dependence, shown in Fig. 3, so for this analysis we refit the data, multiplying the timing likelihood from Eq. 1 by a one-dimensional prior in θ containing the information in Fig. 3 [15]. To keep the computational load to a reasonable level, marginalization of the track position parameters (x, y, z) was not performed; the posterior was simply maximized. Including this prior information reduced the rate of misreconstructions in the 1997 data set by a factor of approximately 410 compared to the timing likelihood fit.

However, the results of the Bayesian fit were not all desirable. The number of events (mis)reconstructed as upgoing was more than an order of magnitude higher than expected based on simulations of atmospheric

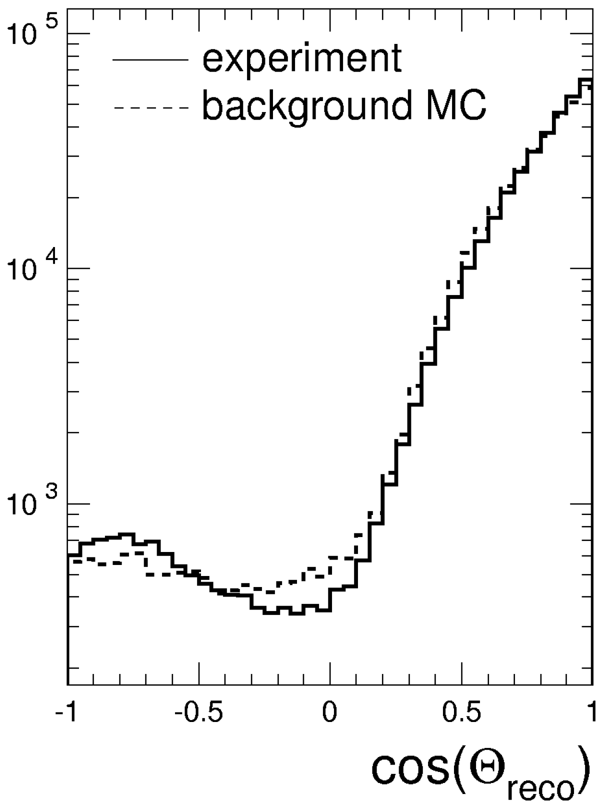

FIG. 6: The reconstructed zenith angle distribution of AMANDA muons, based on the likelihood fit described in the text. Misreconstruction of downgoing atmospheric muons as upgoing neutrino-induced muons is clearly problematic.

muons (which were themselves expected to be an order of magnitude more numerous than atmospheric neutrino events). Interestingly, the distribution of the depths of these misreconstructed events exhibited a pronounced structure, as shown in Fig. 8. Similar asymmetry was also seen in the horizontal distribution of these events.

Extensive investigation of these anomalous events resulted in the discovery that they were, at least in the main, induced by cross talk in the detector. Downgoing muons occasionally emit bright pulses of light through stochastic processes such as bremsstrahlung and pair production, and if the muon is slightly outside the detector it is possible to see the (approximately spherical) light from the bright stochastic event, but not the continuous Cherenkov light. The anomalous events were typical of such simulated muons, except that the high amplitude pulses created cross talk in nearby channels; see Fig. 9.

The timing calibration of the detector resulted in the cross talk pulse being projected to an earlier time than the pulse that induced it, due to the longer cable length to the cross talk channel. This produced an apparently upgoing chronology of hits that fooled the reconstruction algorithm if the spacing between the cross talk and the real hits was just so. (Presumably the anomalous events in Fig. 8 were only the remnant of a much larger class of events with cross talk, the majority of which did not mislead the reconstruction program.) The structure in Fig. 8 is due to a few specific channels with high levels of cross talk. Eliminating these channels from the data stream, and applying some additional cross talk suppression algorithms, the data were refit, with the result seen in Fig. 10. Another, rarer, class of instrumental background, believed to be due to noise in the high voltage supplies, was also discovered and removed from this data set [16]. These events had a characteristic "hollow" topology, with numerous hits on the outer strings but none on the inner strings, which had a higher discriminator threshold.

In the end, quality cuts similar to those in the maximum-likelihood analysis had to be applied to remove the background events from instrumental effects and from downgoing muons [12, 16]. Fig. 11 shows the

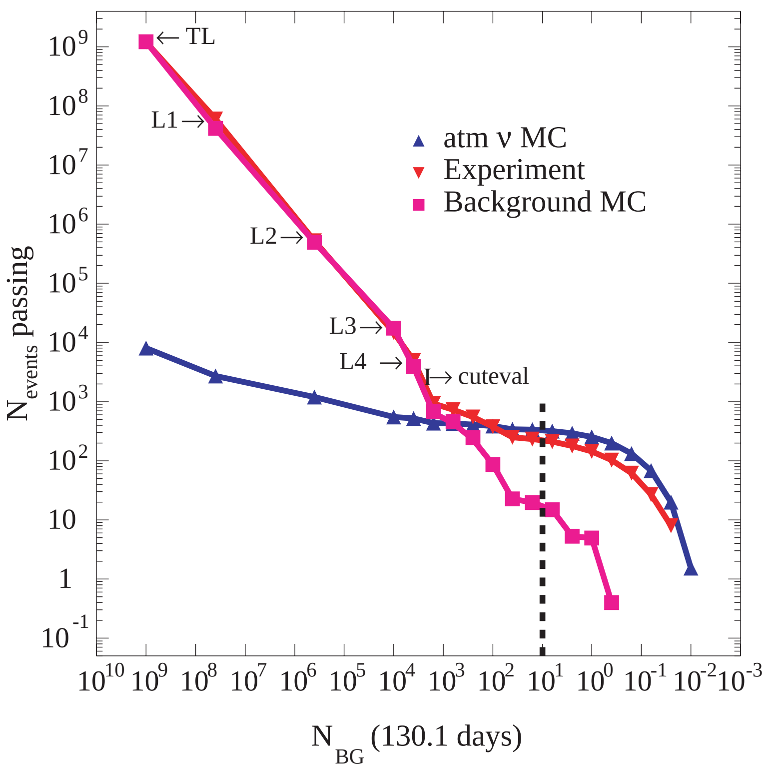

FIG. 7: The number of events surviving the first analysis as cuts are tightened. Note that the background Monte Carlo (simulated misreconstructed downgoing muons) and the data are in good agreement at all levels, until the background are reduced below the level of the signal at a rejection level of 10^{-6}.

effect of progressive tightening of those cuts, in analogy to Fig. 7. Above event quality of 6 or 7, the depth distribution is in good agreement with expectations from the Monte Carlo. Figure 11 shows but the benefits and drawbacks of the Bayesian approach; the rejection level required from the cuts is much smaller than in Fig. 7, but the agreement between data and Monte Carlo is much poorer due to the confusion of the Bayesian fitter by instrumental backgrounds.

IV. CONCLUSIONS

It is interesting to compare the two approaches: the Bayesian fit greatly reduced the need for quality cuts to reject misreconstructed events, but it was only effective against the known backgrounds. The analysis which relied more heavily on cuts, by contrast, was much less vulnerable to these instrumental effects; the more extensive set of cuts selecting "high quality" tracks were effective not only against simulated backgrounds that were understood, but also against instrumental effects that were not. In that analysis, the anomalous depth-dependent events that formed the dominant background to the Bayesian analysis were observed, but the numbers were small compared to the background from "normal" misreconstructed muons, and they were removed with general event-quality cuts (rather than through cleaning of the data stream). The "hollow" events, probably due to oscillations in the high voltage supply, were rejected by the cuts before they became detectable.

Acknowledgments

AMANDA is supported by the following agencies: U.S. National Science Foundation, Office of Polar Programs; U.S. National Science Foundation, Physics Division; University of Wisconsin Alumni Research

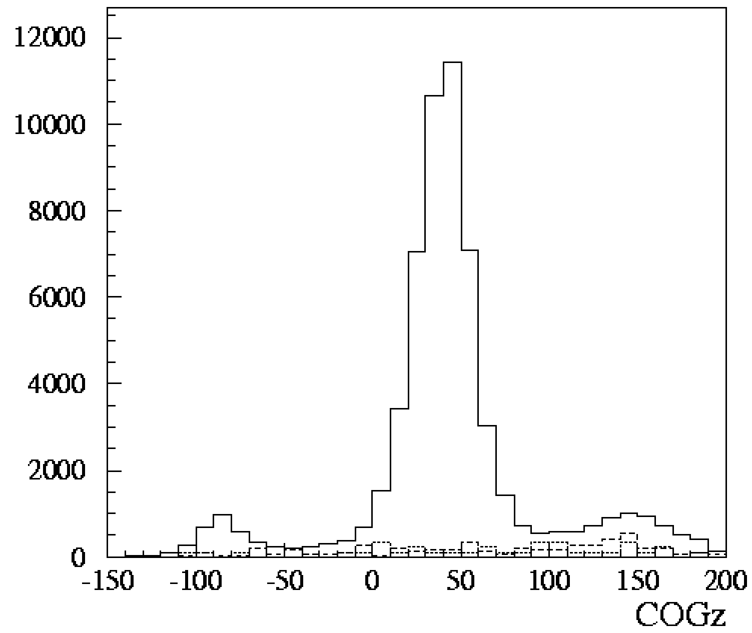

FIG. 8: The distribution of depths of the center of gravity of events reconstructed as upgoing by the Bayesian fitter. The solid line shows the observed data ($5.8 \cdot 10^4$ events), the dashed and dotted lines two Monte Carlo predictions for misreconstructed downgoing atmospheric muons (4–$5 \cdot 10^3$ events). An unexpected class of background at characteristic depths completely dominates the simulated backgrounds.

Foundation; U.S. Department of Energy; Swedish Natural Science Research Council; Swedish Polar Research Secretariat; Knut and Alice Wallenberg Foundation, Sweden; German Ministry for Education and Research; U.S. National Energy Research Scientific Computing Center (supported by the Office of Energy Research of the U.S. Department of Energy); UC-Irvine AENEAS Supercomputer Facility; Deutsche Forschungsgemeinschaft (DFG). D.F. Cowen acknowledges the support of the NSF CAREER program and C. Pérez de los Heros acknowledges support from the EU 4th framework of Training and Mobility of Researchers.

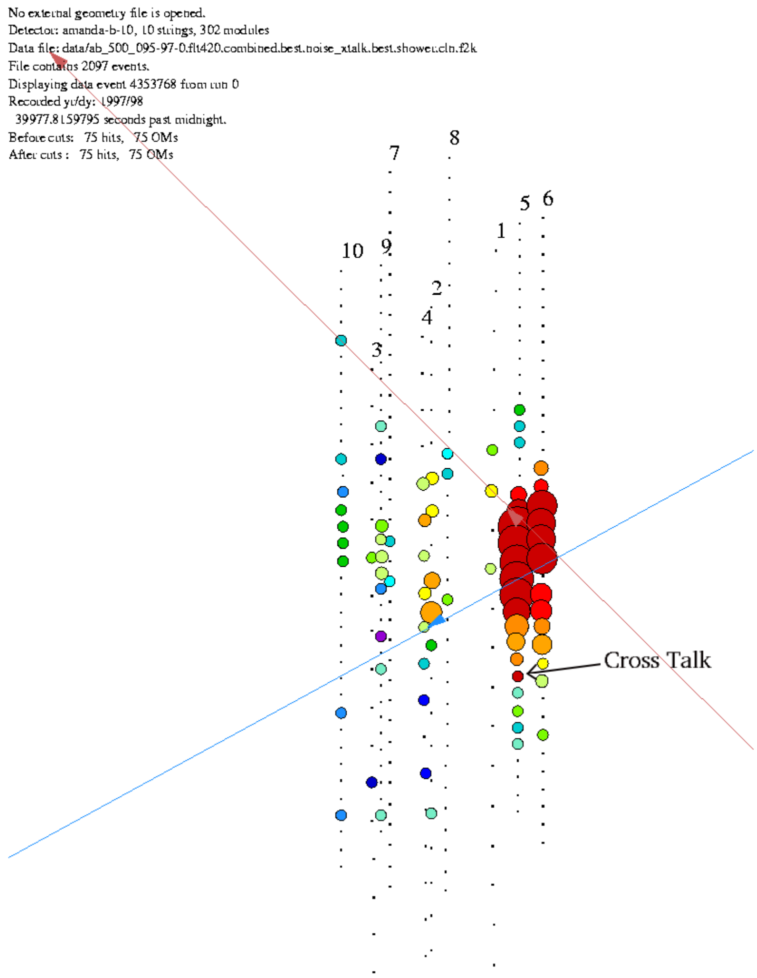

FIG. 9: A typical event from the central peak of Fig. 8. Cross talk in the indicated channel, induced by the high amplitudes in channels just above it, has misled the reconstruction.

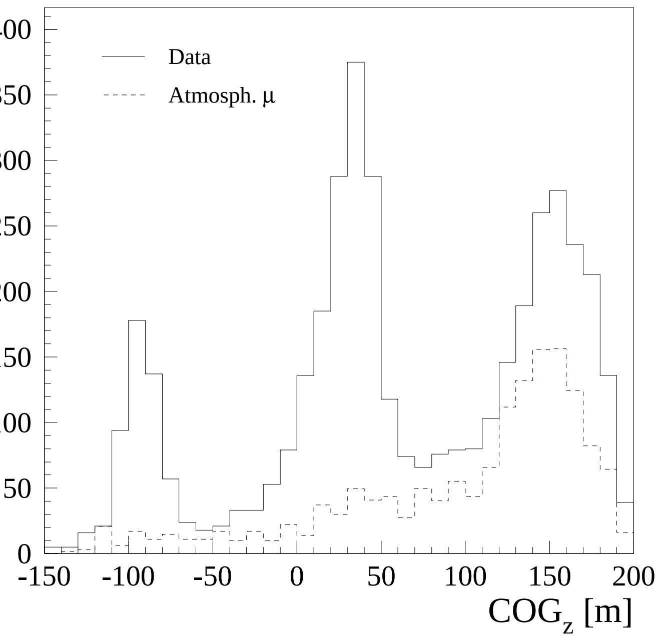

FIG. 10: The distribution of depths of the center of gravity of events reconstructed as upgoing by the Bayesian fitter, after hits due to cross talk and spurious events caused by oscillating high voltage levels were removed from the data stream. The anomalous events have been much reduced, though not completely removed; some quality cuts are required to reject the remnants.

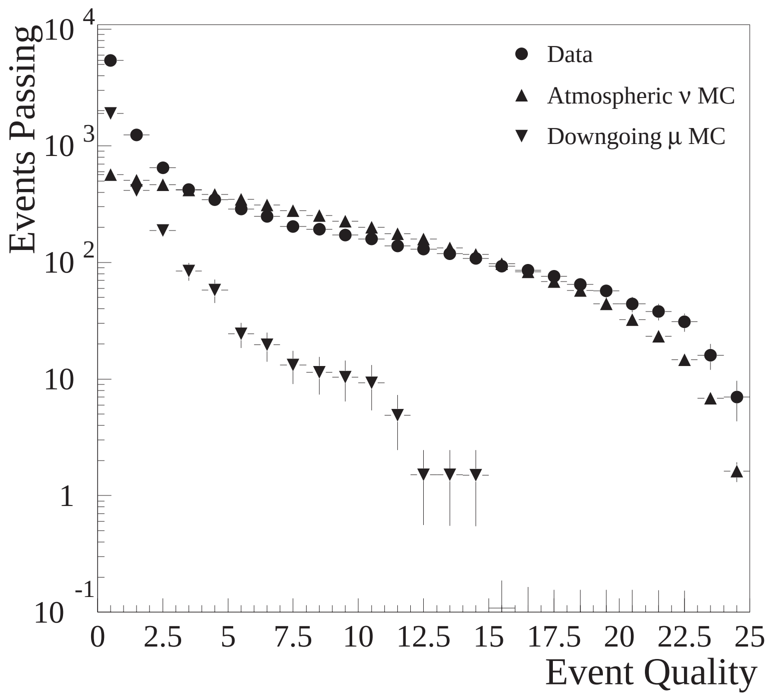

FIG. 11: The number of events surviving the second analysis as cuts are tightened. Quality of $Q = 0$ corresponds to events reconstructed as upgoing after cross talk and other instrumental effects were removed from the data stream; without such cleaning approximately 10 times as many events would be reconstructed as upgoing before cuts.

[1] K. Woschnagg (for the AMANDA Collaboration), in *Proceedings of the 26th International Cosmic Ray Conference* (IUPAP, Salt Lake City, Utah, 1999), Vol. 2, pp. 200–203.
[2] P. B. Price, K. Woschnagg, and D. Chrikin, Geophys. Res. Lett. **27**, 2129 (2000).
[3] B. Wiebel-Sooth and P. L. Biermann, *Landolt-Börnstein: Numerical Data and Functional Relationships in Science and Technology*, Vol. VI 3C of *New Series* (Springer-Verlag, Berlin-Heidelberg, 1998), chapter 7.6, pp. 37–90.
[4] D. Heck *et al.*, Report FZKA 6019, Forschungszentrum Karlsruhe, Karlsruhe, Germany (unpublished).
[5] W. Lohmann, R. Kopp, and R. Voss, Preprint CERN–85–03, Geneva, Switzerland (unpublished).
[6] R. Kopp, W. Lohmann, and R. Voss, MUDEDX: Parametrization and Monte Carlo generation of energy loss of high energy muons (1–10000 GeV); for astrophysicists up to 100000 GeV, Version 2.02, 1995, private communication.
[7] A. Karle, in *Simulation and Analysis Methods for Large Neutrino Telescopes* (DESY, Zeuthen, Germany, 1998), pp. 174–185, DESY-PROC–1999–01.
[8] S. Hundertmark, Ph.D. thesis, Humboldt Universität zu Berlin, Berlin, Germany, 1999, available at URL http://amanda.berkeley.edu/manuscripts/.
[9] P. Lipari, Astrop. Phys. **1**, 195 (1993).
[10] G. C. Hill, Astrop. Phys. **6**, 215 (1997).
[11] G. C. Hill, Ph.D. thesis, University of Adelaide, Adelaide, Australia, 1996.
[12] X. Bai *et al.*, *Observation of High Energy Atmospheric Neutrinos with the Antarctic Muon and Neutrino Detector Array*, submitted to Phys. Rev. D.
[13] C. Wiebusch, in *Simulation and Analysis Methods for Large Neutrino Telescopes* (DESY, Zeuthen, Germany, 1998), pp. 302–316, DESY-PROC–1999–01.
[14] M. Gaug, Diploma thesis, Humboldt Universität zu Berlin, Berlin, Germany, 2001, DESY-THESIS–2001–022, available at URL http://amanda.berkeley.edu/manuscripts/.
[15] G. C. Hill, in *Proceedings of the 27th International Cosmic Ray Conference* (Copernicus Gesellschaft, Hamburg, Germany, 2001), Vol. 3, pp. 1279–1282.
[16] T. R. DeYoung, Ph.D. thesis, University of Wisconsin, Madison, 2001, available at URL http://amanda.berkeley.edu/manuscripts/.